BJA

British Journal of Anaesthesia, xxx (xxx): xxx (xxxx)

doi: 10.1016/j.bja.2020.09.047
Advance Access Publication Date: xxx
Laboratory Investigation

LABORATORY INVESTIGATION

Minimising exposure to droplet and aerosolised pathogens: a computational fluid dynamics study

Paolo Perella[1,*], Mohammad Tabarra[2], Ertan Hataysal[2], Amir Pournasr[2] and Ian Renfrew[3]

[1]Department of Anaesthesia & Perioperative Medicine, Royal London Hospital, Barts Health NHS Trust, London, UK, [2]Arup, London, UK and [3]Department of Interventional Radiology, Royal London Hospital, Barts Health NHS Trust, London, UK

*Corresponding author. E-mail: paolo.perella1@nhs.net

Abstract

Background: Hazardous pathogens are spread in either droplets or aerosols produced during aerosol-generating procedures (AGP). Adjuncts minimising exposure of healthcare workers to hazardous pathogens released during AGP may be beneficial. We used state-of-the-art computational fluid dynamics (CFD) modelling to optimise the performance of a custom-designed shield.

Methods: We modelled airflow patterns and trajectories of particles (size range 1–500 μm) emitted during a typical cough using CFD (ANSYS Fluent software, Canonsburg, PA, USA), in the presence and absence of a protective shield enclosing the head of a patient. We modelled the effect of different shield designs, suction tube position, and suction flow rate on particle escape from the shield.

Results: Use of the shield prevented escape of 99.1–100% of particles, which were either trapped on the shield walls (16–21%) or extracted via suction (79–82%). At most, 0.9% particles remained floating inside the shield. Suction flow rates (40–160 L min^{-1}) had no effect on the final location of particles in a closed system. Particle removal from within the shield was optimal when a suction catheter was placed vertically next to the head of the patient. Addition of multiple openings in the shield reduced the purging performance from 99% at 160 L min^{-1} to 67% at 40 L min^{-1}.

Conclusion: CFD modelling provides information to guide optimisation of the efficient removal of hazardous pathogens released during AGP from a custom-designed shield. These data are essential to establish before clinical use, pragmatic clinical trials, or both.

Keywords: aerosol-generating procedure; airway management; computational fluid dynamics; COVID-19; infection prevention and control; personal protective equipment; SARS-CoV-2; viruses

Editor's key points

- Advanced modelling techniques established in engineering are beginning to be applied in the medical field.
- In this study, the design of a shield to protect personnel in the vicinity of aerosol-generating procedures was modelled and optimised using computational fluid dynamics.
- Quantitative data from this study support the potential of such barriers to reduce environmental and personal biocontamination. As with all new equipment, to ensure safe and proper use, familiarity and adequate training are key.

Recevied: 1 June 2020 **Accepted:** 19 September 2020

Hazardous respiratory pathogens are transmitted in droplet form, aerosols, or by fomite deposition on surfaces.[1] Minimising the number of pathogens present in each transmission route will reduce potential exposure of healthcare workers (HCWs) to dangerous pathogens, including coronavirus disease 2019 (COVID-19). Coughing releases droplets and aerosolised particles with varied diameters and speeds[2] which settle on local surfaces (droplets) or remain aerosolised. Understanding the physics of droplets and airflow can aid the design and guide use of equipment and systems to protect staff and populations against transmissible disease. Computational fluid dynamics (CFD) is a specialist area of mathematics and fluid mechanics used to solve complex engineering problems in industries including aerospace, aviation, and construction. CFD has been used to model cardiorespiratory therapies (e.g. right ventricular assist devices[3] and the design of operating theatres[4]). The predictive success of CFD modelling has obviated the reliance on wind tunnel testing in aviation and racing car design. CFD has also been used successfully in modelling biocontamination. The performance of CFD in predicting simulated aerosolised microbial (*Bacillus licheniformis/aerius*) deposition matched the final location of actual microbes on the internal surfaces of a spacecraft.[5]

To date, the effect of using shields to minimise aerosol contamination in aerosol-generating procedures (AGPs) has not been rigorously tested. We used CFD modelling to test and optimise the performance of a protective shield designed to minimise the spread of droplets and smaller particles produced during AGP, an essential prerequisite before clinical use, the assessment of such devices in pragmatic clinical trials, or both.

Methods

Shield design

In collaboration with Rolls-Royce and the Manufacturing Technology Centre (MTC), we designed a shield to reduce both HCW exposure and local environmental contamination (Fig. 1). The shield is lightweight (4 kg) and easy to manoeuvre. Access ports on each side and vertical access ports are covered by overlapping silicone which forms a seal during use (Fig. 1). The silicone flaps are soft to avoid damaging personal protective equipment (PPE) worn by the operators. A silicone curtain lies over the entrance to the shield, containing both droplets and aerosols within the shield. At the base, 5 cm ports on each side enable suction and ventilation tubing to be maintained at all times and closed loop ventilation to continue once the shield is removed. Further details and video can be found in the Supplementary material. When empty, the shield has a volume of 142.8 L, which reduces to 108 L once the shield is placed over a patient. With an extraction rate of 40 L min^{-1}, 22 air changes per hour (ach) are achieved, rising to 89 ach at an extraction rate of 160 L min^{-1}. Given such large air change inside the box relative to the room, ambient air is drawn into the box. Experiments 1–3 were modelled on the assumption that ambient pressure around the box was 1 atm. In Experiment 4, a room of dimensions 4 m×4.5 m×3.1 m, with air change rate of 10 ach and ambient temperature of 23°C, was modelled (see Supplementary material for further details).

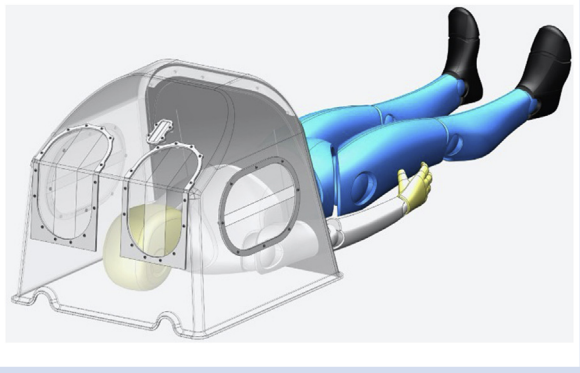

Fig 1. Polyethylene terephthalate glycol-modified (PETG) vacuum formed shield with overlapping silicone access ports. The overlaps for the operator are vertical and horizontal for the assistant to maximise the operator's arm freedom and movement.

Supplementary data related to this article can be found online at https://doi.org/10.1016/j.bja.2020.09.047

Computational fluid dynamics

We used ANSYS Fluent software, Canonsburg, PA,USA[6] to perform CFD modelling of aerosol and droplet dispersion. A total of 1000 particles ranging in size from 1 to 500 μm, were modelled during an initial cough followed by a normal breath.[7] In addition to the standard Navier-Stokes equations governing the three-dimensional features of the fluid (conservation of mass, momentum, and energy), the simulation also uses a Discrete Phase Model that tracks the individual particles in Lagrangian coordinates.[8] The interaction of the particles with the airflow is modelled as a one-way coupling and applied as a post-processing exercise. This means the flow affects the momentum and energy of the particles, but the surrounding fluid flow remains unaffected by the motion of particles.

Particle paths are determined by their size. Heavier particles have more momentum and therefore behave under projectile motion, travelling until they are trapped by a surface. Lighter particles are affected by velocity streamlines, circulating until either encountering a surface or being extracted. Parameters used by the model include ambient temperature, breath temperature, and cough cone angle detailed in the Supplementary material.

Experimental modelling

We first modelled the spread of droplets and aerosols after a cough. We then modelled multiple scenarios to ascertain the optimal design of the shield. Finally, we modelled the dispersion of particles emitted from a cough with the shield and without the shield in a standard sized side room.

Experiment 1: suction tube position

To determine the effect and optimal position of suction within the box, we placed a suction tube modelled on a typical Yankauer sucker, either on the patient's chest or vertically aligned and in-line with the patient's head. The model was run in each of these positions at a suction flow rate of 40 L min^{-1}. Figure 2 shows particle size, streamline velocity, and position of trapped particles (see Supplementary material for videos) (Fig. 2).

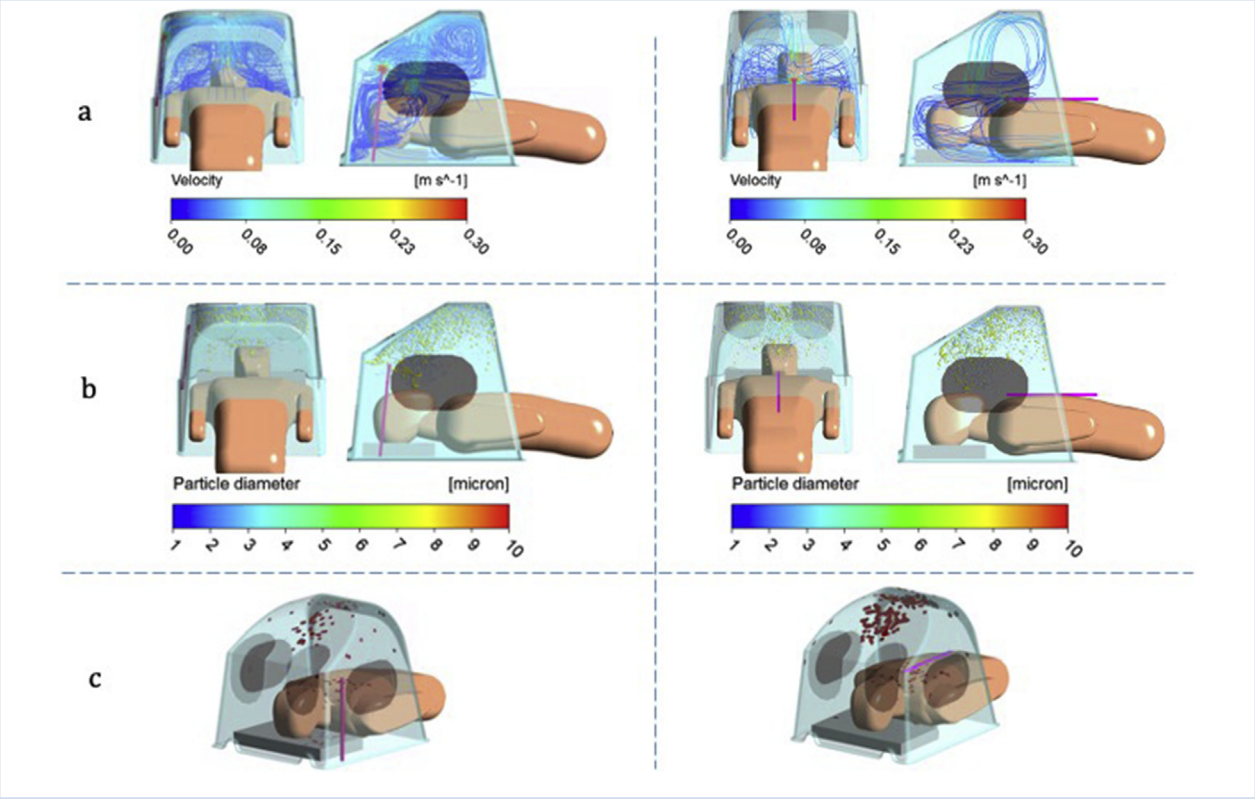

Fig 2. Computational fluid dynamics model with suction placed either vertically and in-line with the patient's head (left) or on the chest (right). (a) Airborne cough particle tracker, (b) velocity streamlines from pressure outlet, and (c) trapped particles on internal shield surfaces.

Experiment 2: effect of additional openings

The shield is designed to allow ambient air to be drawn in around gaps in the curtain which lies over the torso/upper abdomen of the patient, allowing entrainment of air and extraction of box environment through the suction. If the shield is used to perform procedures, further air is likely to enter and there is potential for aerosol to escape via gaps created by the operator's arms (Fig. 3). We modelled the shield without additional openings, and a worst case scenario analysis with all openings patent.

Experiment 3: suction flow rate

Suction flow rate depends on the amount of negative pressure produced by the vacuum source, the resistance of the suction system, and the viscosity of the substance (in this case, air). We modelled a range of suction values (40–160 L min^{-1}) to assess the impact of suction rate on the performance of the shield. We also modelled the effect of these suction ranges with and without additional openings as detailed in Experiment 2.

Experiment 4: presence *vs* absence of shield

We modelled presence of the shield at the lowest suction rate (40 L min^{-1}) with the maximum number of openings patent (worst case scenario) *vs* no shield, in a room measuring 4 m×4.5 m×3.1 m with an air change rate of 10 ach[9] and an ambient temperature of 23°C. Cough particle velocity was 5 ms^{-1} and cough cone angle was 30 degrees.[10,11] Supply and exhaust grills were positioned as per pictures in the Supplementary material. We modelled this scenario with three staff positioned around the patient.

Results

Experiment 1: suction tube position

The position of the Yankauer suction tip within the shield altered the air flow. With the suction placed on the patient's chest, after 500 s, 31% particles were trapped on the shield wall, 56% particles were extracted through the suction tube, 7% remained floating within the box, and 6% escaped. With the suction catheter placed vertically, in line with patient's head, fewer particles were extracted and more particles became trapped on the patient's body and shield walls as the air was drawn towards the patient's chest. With the suction placed in line with the patient's head, 23% more particles were extracted through the suction tube, and ~1% remained floating within the shield (Fig. 4).

Experiment 2: suction flow rate

With the shield placed on the patient, the number of particles escaping the box was negligible over a range of suction flow rates from 40 to 160 L min^{-1} with 99% of particles being

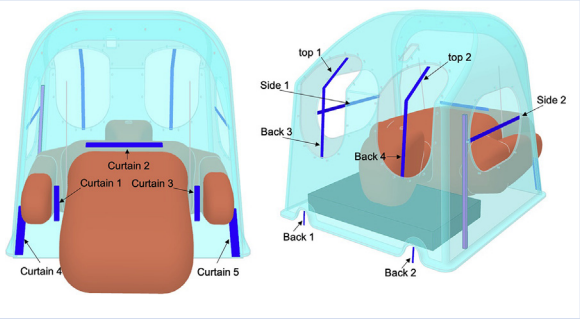

Fig 3. Location of potential openings in shield: back 1 and 2 are ports for ventilation tubing and suction. All other potential openings are covered with silicone flaps. Air enters if these flaps are opened for access to the patient.

removed via suction or trapped on the walls of the shield (Fig. 5, left panel).

Experiment 3: impact of incomplete seals

With all openings patent, particle escape from the shield ranged from 1% to 33% depending on the suction flow rate (Fig. 5, right panel). The proportion of particles trapped on the walls is less affected by incomplete seals (16–20% in the closed model, 19–22% in the open model). The proportions of particles by size, escaping from each opening, in the open and closed models, at varying suction rates can be found in the Supplementary material.

Experiment 4: presence vs absence of shield

Without the shield, larger particles travelled along their trajectory until they landed either on the medical staff or on surfaces in the room. Smaller particles travelled along the paths created by the velocity streamlines from the room ventilation system; these particles circulated in the room until they were either trapped on surfaces inside the room or extracted via room ventilation.

Figure 6 shows the positions of particles, by size, using room parameters outlined in the methods. The shield performance is improved inside the positively pressurised room, keeping more particles contained within as a result of the air flow pattern around the shield and the increased pressure gradient between the room and the shield. Further images are supplied in the Supplementary material showing the distances travelled by aerosolised particles according to their size.

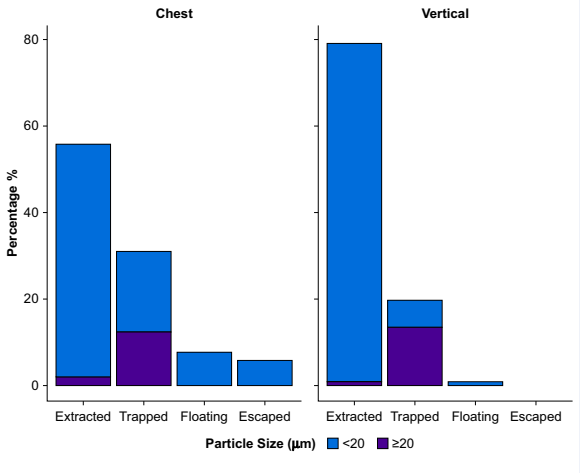

Fig 4. End location of particles after 500 s, according to size and suction position either on the patient's chest (Chest) or vertically, in-line with their head (Vertical). Escaped: escaped perimeter of shield; Extracted: extracted through suction tube; Floating: remaining inside shield in aerosol; Trapped: trapped on internal surface of shield.

Discussion

This is the first study to use CFD to evaluate the effect of a barrier shield on aerosol and droplet trajectories. The CFD study shows this shield is highly effective at removing both droplets and aerosolised particles which would otherwise contaminate the local environment and personnel.

The COVID-19 pandemic has highlighted the risk of transmission via aerosolisation and respiratory secretions. HCWs are at highest risk of contracting infections transmitted in aerosols and droplets when performing AGPs and working in high-risk clinical areas including intensive care, operating theatres, endoscopy, and bronchoscopy units.[12] Up to 4.4% patients with COVID-19 in China were HCWs or individuals who worked in medical facilities.[13] The figure is higher in Italy (10%) and Spain (11.1%).[14,15] Compliance with PPE is advised to reduce transmission rates[16]; however, despite complying with Public Health England guidance, HCWs remain vulnerable to nosocomial transmission.[17] There is uncertainty as to the exact mode of transmission of SARS-CoV-19. Recently published studies add to the argument that significant quantities of virus are present in aerosols generated by the patient, even in the absence of AGPs.[18,19]

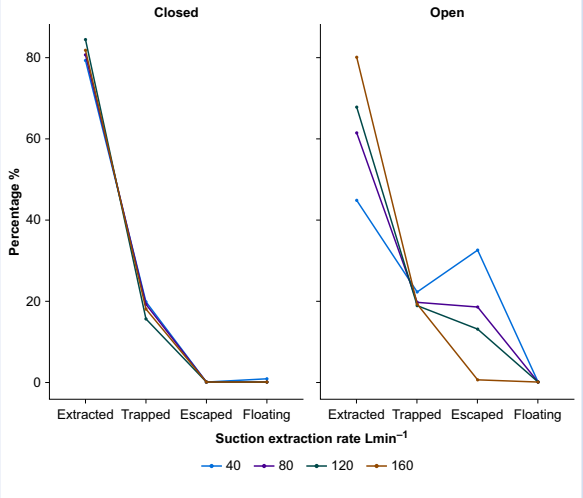

Fig 5. End locations of particles after 500 s in closed model (left panel) and open model—all potential openings fully patent (right panel) according to suction rate.

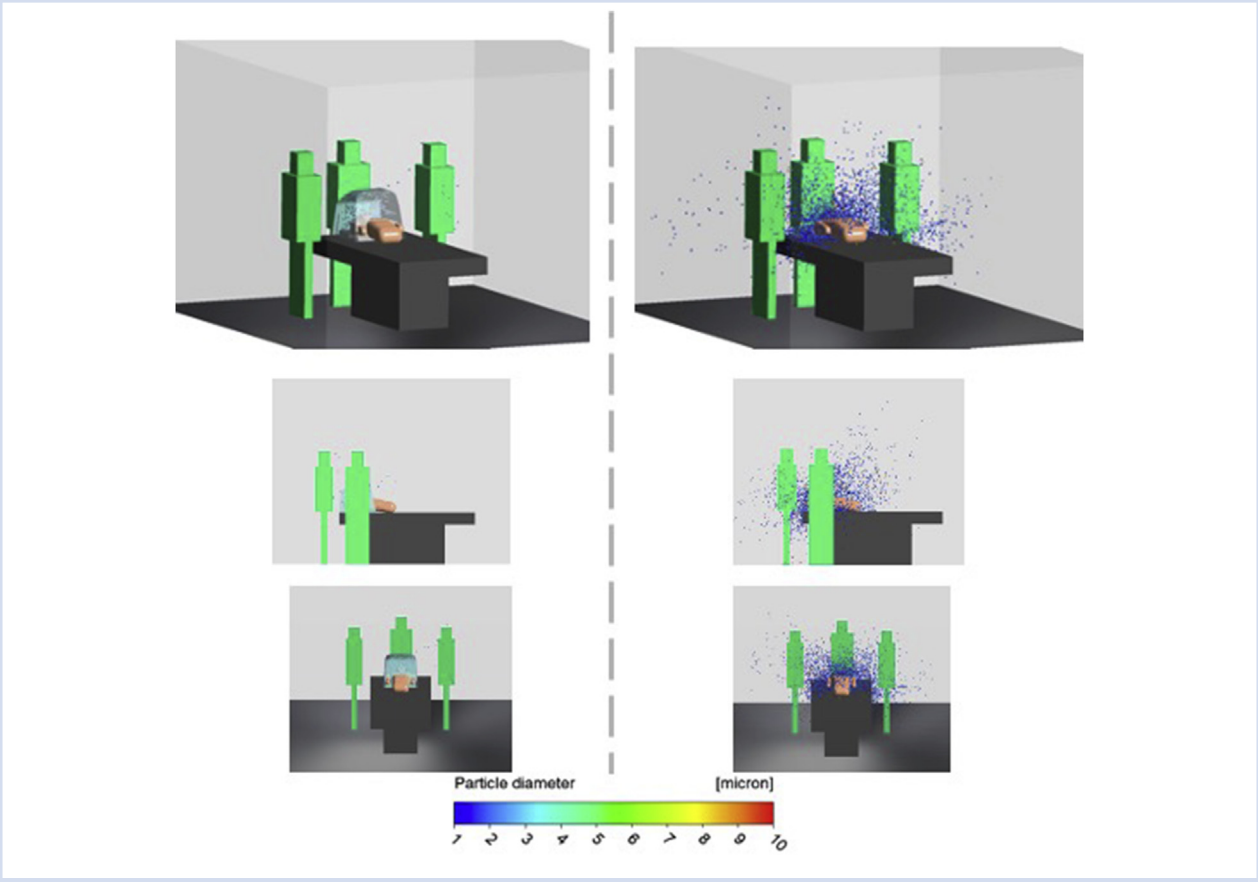

Fig 6. Distribution of particles by size in room with 10 air changes per hour (ach) after a cough then normal breathing. Left panel: modelled with shield on, all potential openings patent and suction inside shield of 40 L min^{-1}. Right panel: same room without shield present.

There is therefore growing interest in, and use of, barrier devices as a method to reduce occupational exposure and potentially nosocomial infections. Similar barrier methods (termed as 'intubation protection box') have been used to compare direct laryngoscopy, videolaryngoscopy, and videolaryngoscopy using a protective intubation box, in an airway mannequin *in vivo*.[20] In this simulated intubation scenario, a mucosal atomisation device was used to simulate a cough and aerosolisation of droplets, which was attached to a 10 ml syringe containing a red dye solution. Although direct and videolaryngoscopy were associated with dye being deposited on the laryngoscopist's face shield, gown, arms, glove, neck, and hair, use of the box reduced the deposition of dye only on the gloves and forearms within the box. No dye was visible on any part of the laryngoscopist located outside the box. Although this approach primarily quantifies the spread of droplets, it is unlikely to characterise the distribution of fine aerosols.

Our study adds quantitative data to support the plausibility of such barriers reducing environmental and personal biocontamination. We suggest such barriers could be used as an extra precaution in addition to gold standard PPE as part of a PPE bundle to reduce nosocomial and occupational infections. These findings reinforce the pressing need for the systematic assessment of new devices that may offer definitive protection before their clinical deployment. We used state-of-the-art CFD modelling, which has a robust track record in complex industrial design that has frequently superseded the need for *in vivo* confirmation. This approach afforded the modelling of a range of scenarios that cannot be replicated *in vivo*. Modelling the distribution and locations of particles in a room beyond the shield depends on factors including, but not limited to room size, ventilation location, rate and turbulence and the position of equipment and personnel within the room. Although these factors vary widely between hospitals and even within hospitals, the exact proportions and final locations of particles will naturally vary. Nonetheless, our study clearly demonstrates the utility of this device in containing infectious matter regardless of the environment in which it is used.

Although our study is limited by not assessing the effect of this shield *in vivo*, we modelled conservatively. We modelled all potential openings fully patent reducing the efficacy of the shield. The seal formed by the silicone flaps around the operator's arms reduces potential openings. Furthermore, it is unlikely that all openings modelled will be patent, for example the airway assistant will either be accessing the patient from right or left rather than both sides. Additionally, when used in a positively pressurised room, the performance is further improved. The results presented in the open model are therefore a worst case scenario. A further limitation is that we did not consider the evaporation of the particles; however, this is likely to decrease the time particles residing within the

shield. Although the extraction of the majority of particles occurred through the suction, use without suction will still trap 97% of droplets produced.

As with all new equipment, training and familiarity is vital, and all staff involved should be confident in both the theory and practical application. In summary, we provide robust CFD modelling data showing that this custom design shield effectively minimises exposure of HCWs to droplets and aerosols that may transmit hazardous pathogens, and that environmental contamination is reduced. Further clinical assessment is warranted, as the targeted use of such devices may enhance the PPE armamentarium to HCWs globally in preparation for future predicted pandemics.

Authors' contributions

Drafting manuscript: PP
Data analysis: PP, AP
CFD model and figures: MT, EH, AP
Revision and approval of final version of article: all authors

Acknowledgements

Rolls Royce and the Manufacturing Technology Centre were instrumental in the rapid design, development, production, and distribution of the shield. Andy York, Head of Programmes, Manufacturing Technology, Rolls Royce. Alan Pardoe Partnership Manager, the Manufacturing Technology Centre (MTC), Rolls-Royce. Danny McGee, Chief Engineer, (MTC, Coventry. Multimatic, a global enterprise supplying engineered components, systems, and services to the automotive industry, who developed the vacuum forming tooling for the shield. Aston Martin, for help with distribution of the shields for testing. Edith Blennerhassett Director, Arup, an independent firm of designers, planners, engineers, architects, consultants, and technical specialists who supported this study gratis.

Declarations of interest

Designers/patent holders: PP/IR.

Funding

Arup, through their Community Engagement COVID Response fund. Production of the shield was funded by a grant from Innovate UK.

Appendix A. Supplementary data

Supplementary data to this article can be found online at https://doi.org/10.1016/j.bja.2020.09.047.

References

1. Tellier R, Li Y, Cowling BJ, Tang JW. Recognition of aerosol transmission of infectious agents: a commentary. *BMC Infect Dis* 2019; **19**: 101
2. Yang S, Lee GW, Chen C-M, Wu C-C, Yu K-P. The size and concentration of droplets generated by coughing in human subjects. *J Aerosol Med* 2007; **20**: 484–94
3. Fukamachi K, Saeed D, Massiello AL, et al. Development of DexAide right ventricular assist device: update II. *ASAIO J* 2008; **54**: 589–93
4. Colquhoun J, Partridge L. Computational fluid dynamics applications in hospital ventilation design. *Indoor Built Environ* 2003; **12**: 81–8
5. Salmela A, Kulmala I, Karvinen A, et al. Measurement and simulation of biocontamination in an enclosed habitat. *Aerosol Sci Eng* 2020; **4**: 101–10
6. ANSYS. *ANSYS fluent user's guide, release 2019*. ANSYS; 2020. Available from: www.ansys.com. [Accessed 29 April 2020]
7. Aliabadi AA, Rogak SN, Green SI, Bartlett KH. CFD simulation of human coughs and sneezes: a study in droplet dispersion, heat, and mass transfer. In: *Proceedings of the ASME 2010 international mechanical engineering congress and exposition. Volume 7: fluid flow, heat transfer and thermal systems, parts A and B. Vancouver, BC, Canada: 2010: 1051–60*; 2007
8. Ferziger JH, Perić M, Street RL. *Computational methods for fluid dynamics*. Cham: Springer; 2020
9. Department of Health. *Health technical memorandum 03-01: specialised ventilation for healthcare premises. Part A – design and installation* 2007
10. Tang JW, Settles GS. Images in clinical medicine. Coughing and aerosols. *N Engl J Med* 2008; **359**: e19
11. Dudalski N. *Experimental measurements of human cough airflows from healthy subjects and those infected with respiratory viruses*. Electronic Thesis and Dissertation Repository 2018. p. 5965. Available from: https://ir.lib.uwo.ca/etd/5965. [Accessed 3 November 2020]
12. Tran K, Cimon K, Severn M, Pessoa-Silva CL, Conly J. Aerosol generating procedures and risk of transmission of acute respiratory infections to healthcare workers: a systematic review. *PLoS ONE* 2012; **7**, e35797
13. Zhan M, Qin Y, Xue X, Zhu S. Death from Covid-19 of 23 health care workers in China. *N Engl J Med* 2020; **382**: 2267–8
14. Stituto Superiore di Sanità. Integrated surveillance of COVID-19 in Italy. Available from: https://www.epicentro.iss.it/coronavirus/bollettino/Infografica_19marzo%20ENG.pdf (accessed 3 November 2020).
15. Suárez-García I, Martínez de Aramayona López MJ, Sáez Vicente A, Lobo P. SARS-CoV-2 infection among healthcare workers in a hospital in Madrid, Spain. *J Hosp Infect* 2020; **106**: 357–63
16. Lockhart SL, Duggan LV, Wax RS, Saad S, Grocott HP. Personal protective equipment (PPE) for both anesthesiologists and other airway managers: principles and practice during the COVID-19 pandemic. *Can J Anaesth* 2020; **67**: 1005–15
17. Heij R, Steel AG, Young PJ. Testing for coverage from personal protective equipment. *Anaesthesia* 2020; **75**: 966–7
18. Fennelly KP. Particle sizes of infectious aerosols: implications for infection control. *Lancet Respir Med* 2020; **8**: 914–24
19. Lednicky John A, Lauzardo Michael, Fan Z Hugh, et al. Viable SARS-CoV-2 in the air of a hospital room with COVID-19 patients. *Int J Infect Dis* Nov 2020; **100**: 476–82
20. Yang SS, Zhang M, Chong JJ. Comparison of three tracheal intubation methods for reducing droplet spread for use in COVID-19 patients. *Br J Anaesth* 2020; **125**. e190–1

Handling editor: Jonathan Hardman